https://doi.org/10.17163/abyaups.49.377

Analyze Characteristic Curves of People Biomechanical Conditions with Knee Osteoarthritis using Inertial Sensors on Flat Surfaces

Eduardo Cóndor
Universidad Politécnica Salesiana, Ecuador

José Condolo
Universidad Politécnica Salesiana, Ecuador

Víctor H. Cabrera–Moreta
Universidad Politécnica Salesiana, Ecuador
Orcid: https://orcid.org/0000–0001–9482–5705

Introduction

In the past few years, there has been a rise in the utilization of inertial sensors for gait analysis. The most notable research in this field is summarized in Table 1. These studies demonstrate the effective implementation of inertial sensor systems for measuring knee osteoarthritis in patients, which has sparked even greater interest in utilizing such systems for clinical research. Patient–reported outcome measures (PROMs) and gait analysis are commonly employed methods for assessing functionality.

PROMs, although practical and widely available, suffer from substantial limitations in terms of function measurements (Renata *et al.,* 2012).

Figure 1

Complete gait cycle (Martínez et al., 2018). Standard analysis of gait (Calderón, 2016)

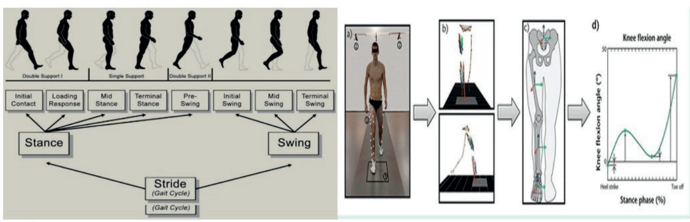

There is ample evidence of differences in spatiotemporal parameters between patients with severe knee osteoarthritis and healthy controls (for a review, see Straw *et al.* (2010) and Calderón (2016)). However, the time requirements and the need for specialized personnel and dedicated gait laboratories with camera systems make laboratory–based gait analysis very expensive (Calderón, 2016).

According to the figure, it can be shown that the: (a) Subject with reflective markers walks in a gait laboratory equipped with a camera network, (b) camera signals are processed, (c) biomechanical modeling is performed, (d) descriptive modeling is performed to quantify joint kinetics and kinematics (Calderon, 2016).

Gait analysis establishes movement patterns that identify pathologies and events that can predict falls. To establish a real–time measurement system, a FPGA (Field–Programmable Gate Array) and four inertial sensors were employed. Each lower limb was equipped with an accelerometer positioned on the thigh to estimate the hip angle, while another accelerometer was placed on the leg to estimate the knee angle.

The firmware and software design allowed a maximum delay time, between readings, of 724 μs, achieving a sampling rate of 250 Hz. The computational systems help us to improve the studies, which are pivotal when defining behaviors since it is very helpful in the cause–effect relationships as in this study (Panebianco *et al.,* 2020; Carmenate Milián, 2014).

According to the figure, the most relevant inertial sensors are the gyroscope, accelerometer, and magnetometer, which are used to carry out a suitable study on the behavior and restrictions that may occur in the movement of the object of study. The lightweight portable nature makes inertial sensors an effective tool to be implemented for clinical fall risk assessment and continuous unsupervised home monitoring in addition to outdoor testing (Góngora García, 2003; Aranda Varela, 2018). The error distributions for various gait events and temporal parameters during water walking were influenced by the positioning of the sensor, the target variable, and the computational approach employed. Wearable inertial sensors have been developed lately, based on a set of sensors that are housed in a small device in which a 3D gyroscope, a 3D accelerometer, and a 3D magnetometer are wireless (INEC, 2010).

The methods applied for measuring and evaluating body posture do not manipulate any tissue to be analyzed, so an analysis of body posture is performed in vivo, nuclear magnetic resonance (NMR), computed axial tomography (CAT), dual X–ray absorptiometry (DXA) and plestimography methods because they are used in research and clinical settings (Moreta *et al*., 2023). Carmenate Milián *et al*. (2014) measured the length of the knee of the individual in a seated position taking distance from the vertical to the anterior part of the knee using an anthropometer, where the person is in a forward–facing position with a right angle at the ankles and knees.

Table 1
Relevant Research

Authors	Analysis	Type of Patients
Broche *et al.* (Aranda Varela, 2018)	Gait asymmetry in biomechanical behavior of hip joints.	Handicapped Patients
Antwi–Afari and Li (Costa, 2015)	Fall risk assessment of construction workers based on biomechanical stability parameter.	Healthy patients.
Tse *et al*. (Carmenate Milián *et al.*, 2014)	Biomechanics of gait in the influence of foot posture when designing lateral wedge insole with variable stiffness support.	Healthy patients aged 23–34 years
Romero and Barrios (Góngora García *et al.*, 2003)	Gait biomechanics.	Patients with motor disability

Method

Protocol and parameters

Figure 2
Inertial sensors´ location

(Calderón, 2018)

The recruited individuals will perform the 10–meter walk test (10MWT), in a straight line at their own pace and barefoot, a test used by Cleland *et al*. (2019) and Nikaido *et al*. (2019). For the analysis, 7 inertial sensors will be used in the area of the pelvis, quadriceps, anterior tibialis, and feet, as shown in Figure 2. Three tests per participant will be performed on a flat tile surface, to rule out possible errors at the time of averaging the characteristic curves obtained from the sensors. Data transfer from each sensor was done via wireless connection to the Awinda station unit which includes a USB cable to be connected to a laptop to store all the collected data in the Xsens MT Manager software.

Data Analysis

The beginning of the measurement on the march is arranged in the first step performed by which there is a contact of the foot with the starting surface and culminates with the forced foot on the final line of the section. All tests were taken into account since they were necessary to have an optimal result.

The sensors have the incremental oriental programming to perform measurements and storage in Euler angles specifically in the rotation in the x, y, and z axis with the names of Roll ϕ, Pitch θ, and Yaw Ψ, respectively (Jouybari *et al*., 2019). The erroneous data generated by the sensors before and after the tests were eliminated to avoid curve deviations, once the data of quadriceps, tibialis, pelvis, and feet were collated to obtain the kinematic angles of the knee in which we resort to Equation 1 implemented by Garza-Ulloa (2018).

$$\theta knee = \theta shank + (180 - \theta thigh) \quad (1)$$

Where θ_{knee} corresponds to the knee angle, θ_{shank} to the tibialis anterior angle, and θ_{thigh} to the quadriceps angle.

For the refinement of the data obtained, the method of polynomial linear regression by least squares was used, which provides a polynomial function of degree n, with a biomechanical sequence generated that is similar to each of the tests performed on the individuals in the study. To demonstrate how effective polynomial regression can be, it is performed using an analysis of the square root of the quadratic error as shown in equation 2.

$$RMSE = \sqrt{\frac{1}{n}\sum_{i=1}^{n}\left(Y_i - \hat{Y}_i\right)^2} \quad (2)$$

To infer in the study, a comparative analysis of the graphs obtained by Calderón–Ulloa (Costa *et al*., 2015; Armas *et al*., 2023; Moreta *et al*., 2023) and the graphs generated by the data obtained through Xsens MTw Awinda sensors was performed.

Participants

It is estimated that approximately 25 % of people over 55 years of age manifest knee pain due to osteoarthritis, so there is a population of 2,239,191 inhabitants of which 25 % are 559,797 people according to the 2010 census (Di, 2020).

The tests were performed on 3 individuals (2 women and 1 man) living in the Metropolitan District of Quito, Pichincha, Ecuador who were previously diagnosed with osteoarthritis of the knee. The parameters established for each subject were weight, height, age, and body mass index (BMI), data specified in Table 1. Due to the anthropometry of each participant, the characteristic curves obtained were different.

Table 2
Participants

P	Gender M/F	Weight [kg]	Height [m]	Age [years]	BMI [kg/m²]
1	F	78	1.68	68	27.6
2	F	78.95	1.51	66	34.6
3	M	65.04	1.50	67	28.9

Results

The data obtained by the IMMUs in the measurement of the gait of the elderly, after the location in the pelvis in the L5 vertebra, tibial quadriceps, and feet, presented several curves which had specific patterns and could be superimposed and compared, However, some of them presented alterations due to noises present at the beginning and end of the tests, so those values were eliminated and not taken into account, even so, when proceeding with the tests, two more tests were performed to each one of the study subjects to ensure that the data being obtained were adequate to solve the noises present at the beginning and end of each test performed.

The people who underwent the study are older adults whose age ranges from 65 years and older, which is the age with the highest rate of problems with osteoarthritis in knees which directly influences their gait cycle. There are considerable differences in the rotation and pelvic obliquity in which can be seen the pattern of a person without osteoarthritis in knees compared to one that does, considering that there is a pattern of similarity with the same. Each person in the study had from 9 to 18 samples, considering each limb in which the sensor is located, i.e., feet, quadriceps, tibial, pelvis, and knees, the latter have fewer samples due to the calculation for obtaining its angle, thus reducing the number of samples.

The patterns obtained are compared with the study subject P3 for being the person who has a not–so–advanced level of knee osteoarthritis and the subject P2 who has osteoarthritis in the advanced stage determined. The data of P2 vary more to P1 and P3. Using MATLAB software, the data obtained during the tests performed on the study subjects are outlined, and each person was assigned a color for its distinction, thus generating average curves to perform the polynomial regression.

The number of similar samples obtained are from 10 to 16 samples for the flexion–extension of the right quadriceps in the sagittal plane. The maximum value was established at 3.59º and 6.01º, respectively in P1 and P3 while P2 has a value of 20º as maximum and a minimum of –103, 30º. The flexion and extension of the left quadriceps in the sagittal plane were determined from 15 to 18 samples as well as the right quadriceps, the maximum angle obtained is 13º for P3 and the minimum –130, 6º for P2.

There are 10 to 12 samples in the pelvic obliquity for P1 and P3 which have a global pattern. P2 by not having enough samples due to the elimination of a test which had many erroneous data was not considered, even so, we can determine the maximum and minimum angle that P1 has with 59.6º and –177.9º, respectively.

For the internal and external rotation that occurs in the pelvis during gait activity, 4 to 10 samples were obtained. There were two different patterns in which we have P1, P3, and P2, which present positive and negative ranges P1, P2, and P3 establishing a wide variation between their maximum and minimum, considering P1 as the general range that includes P2 and P3 with a maximum angle of 34.24 º and a minimum angle of –67.37º. The flexion and extension angles of the right tibialis during gait were obtained between 12 to 13 similar samples in the sagittal plane, the maximum angle value is 31.85° for P1 and the minimum value is –168.3°, –176.3° for P1 and P2, respectively.

In left tibial flexion and extension, 12 to 18 similar samples were obtained for each subject, and the maximum angle value is 22.05° for P1 and the minimum value is –179.6° for P2.

The number of samples obtained for quadriceps and tibialis determines the number of samples that can be obtained for knees. By using Equation 1, the samples for right knee flexion and extension are in the range of 10 for P1, P2, and P3, the maximum value of the angle is in 206.3° and the minimum value set is –41.41° for P1 and P2, P3 has a maximum angle of 91.46º and a minimum angle of –37.94º. As for left knee flexion and extension these were determined from 12 samples, the maximum angle value is 155.8° for P2 and the minimum value is –55.23°, for P1 and P2. P3 has a maximum angular value of 91, 46º and a minimum value of –37.94º.

For the angular displacement of the right foot, there are 12 to 14 samples, in which a maximum angle of 27.39º is obtained in P2 and a minimum angle of –69.59º for P1, establishing a clear pattern. For the angular displacement of the left foot, there are 9 to 18 samples, in which a maximum angle of 25.58º is obtained in P2 and a minimum angle of –64º for P1, P2, and P3, establishing a clear pattern.

The value “n” underwent a polynomial regression using the least squares method with the average values of the samples. The regression analysis was conducted in MATLAB software, utilizing polyfit (x, y, n) command to determine the coefficients of the regression polynomial. Additionally, polyval (p, x) command was utilized to evaluate the polynomial p(x) with a degree of n (determined by polyfit) at each point of x.

Figure 4 shows the graphs resulting from the polynomial regression and the confidence interval established at 95 % for each of the regressions performed on the samples of pelvic rotation and obliquity, flexion, and extension of the quadriceps, tibialis, knees, and feet. The acronyms in the legends in each of the graphs are BC for confidence band and AP for least squares approximation.

The polynomial regressions performed have n ranges from the minimum value of 5 for Pelvic obliquity in the sagittal plane for senior P2 and 8 for the angular displacement of the right knee for senior P1, P2, and P3, to a maximum n equal to 16 for the angular displacement of the left ankle for senior P1. The regressions carried out must have a higher n in the tibial and knee to be able to be coupled to the original values obtained using the Xsens MTw Awinda sensors. To evaluate the performance of the polynomial regression, RMSE was performed between the data provided by the sensors and the data yielded by the command polyval(p, x) for the polynomial p(x) of the regression in MATLAB. Table 3 presents the values of the older adults.

Table 3
Root value of root mean square error of polynomial curve fitting

	P1	P2	P 3
Pelvic obliquity	1.58E–08	7.98E–09	2.59E–08
Pelvic rotation	5.99E–08	5.95E–10	2.27E–09
Flex/Ext right quadriceps	4.32E–08	1.59E–06	6.93E–07
Flex/Ext left quadriceps	1.80E–06	8.06E–08	8.04E–06
Flex/Ext right tibialis anterior right	6.60E–09	3.36E–09	7.73E–10
Flex/Ext tibialis anterior left	3.03E–10	7.68E–12	8.54E–10
Flex/Ext right knee	4.98E–10	7.21E–10	4.99E–10
Flex/Ext left knee	7.63E–11	5.87E–10	4.06E–10
Flex/Ext left foot	1.18E–05	1.67E–10	5.45E–10
Right foot	1.69E–08	6.36E–10	2.05E–09

When comparing the data adjusted by least squares provided by the sensors with the data of Calderón and Ulloa (2016), the results are different from the expected, since people with different stages of the disease intervened in the study; however, what is sought is to denote the link that exists between the studies. For this reason, an assessment is made, thus determining the relationship that exists between the databases by applying the Pearson R. correlation coefficient, as seen in Table 3.

The values in Table 4 determine that there is a direct relationship with the group of data evaluated, which is not perfect considering that the people in the study have a disease that makes walking difficult, even so, obtaining values different from zero makes it difficult to state that there is a correlation, with minimum values of 0.07 for pelvic obliquity and 0.09 for flexion and extension of the right anterior tibialis anterior belonging to the older adult P2, who has a more advanced pathology than the rest of the subjects. 0.07 for pelvic obliquity and 0.09 for flexion and extension of the right tibialis anterior belonging to the older adult P2 who has a more advanced pathology than the rest of the study subjects, the maximum values are 0.55 in pelvic obliquity of the older adult P3 and 0.53 in flexion and extension of the left quadriceps of the older adult P1. To reaffirm the similarity granted by the Pearson's relationship coefficient, a statistical distinction of the determination coefficient is performed, and the data are detailed in Table 4.

Figure 3

Comparison of the patterns evaluated in the gait cycle: (a) pelvic obliquity, (b) pelvic rotation, (c) flexion and extension of right quadriceps, (d) flexion and extension of left quadriceps, (e) flexion and extension of right anterior tibialis, (f) flexion and extension of left anterior tibialis, (g) flexion and extension of the right knee and (h) flexion and extension of the left knee

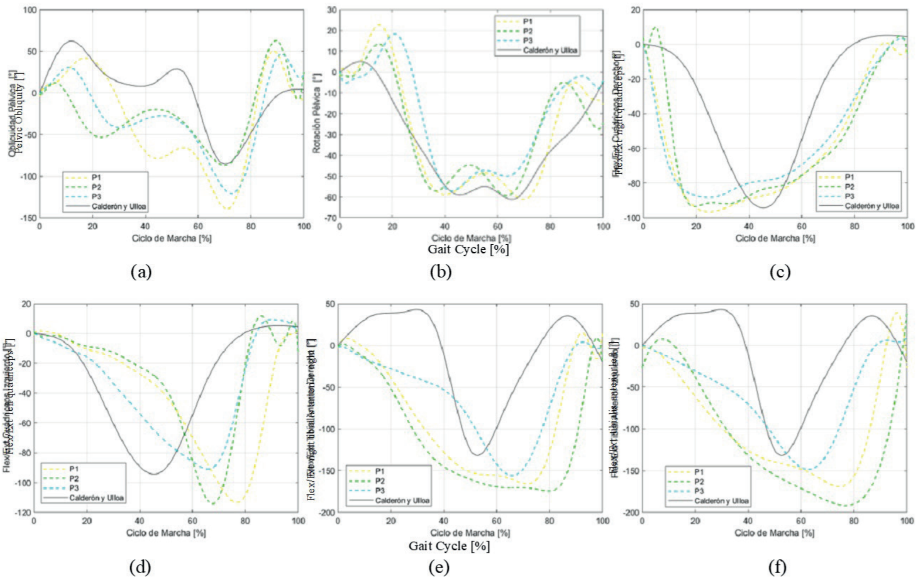

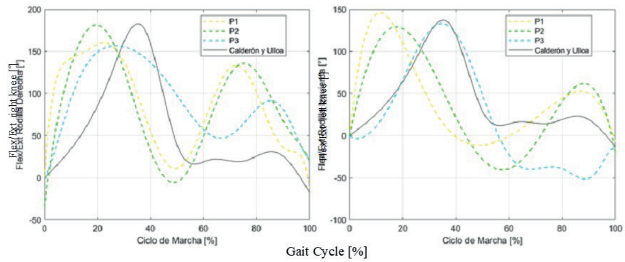

(g) (h)

Table 3
Coefficient

	Pearson's correlation coefficient, R			Coefficient of determination, R2 [%]		
	P1	P2	P3	P1	P2	P3
Pelvic obliquity	–0.32	0.07	–0.55	10.52	0.49	30.55
Pelvic rotation	0.43	0.37	0.33	18.67	14.03	11.35
Flex/Ext right quadriceps	–0.28	0.46	–0.25	7.91	21.53	6.51
Flex/Ext left quadriceps	–0.53	0.20	–0.16	28.67	4.18	2.82
Flex/Ext right tibialis anterior right	–0.32	0.09	0.16	10.81	0.84	2.78
Flex/Ext tibialis anterior left	0.05	–0.29	0.21	0.31	8.77	4.44
Flex/Ext right knee	–0.25	–0.27	–0.26	6.66	7.57	7.01
Flex/Ext left knee	–0.18	–0.30	0.11	3.45	9.32	1.25

The data obtained show that the percentage of 11.35 to 18.67 is the one that presents the greatest similarity found in the pelvic rotation, followed by the pelvic obliquity that has a little similar value of the older adult P2 who has a more advanced stage of the disease, followed by the older adult P1 who has a percentage of 0.31, showing that his left anterior tibial affects the gait in an important way as well as with a percentage of 0.84 of the older adult P2 in the right anterior tibial. The polynomial statistical analysis corroborates the similarity in different parts of the limbs and not in all since the study tends to have a pattern, but not to be equal since the study subjects have a disease which hinders their gait, so the measurements taken by using the Xsens MTw Awinda inertial sensors optimally validate the people involved, as seen in Table 4.

Conclusions

The usefulness of inertial sensors allows recording data of human movements in real-time, thus helping research to be carried out in a laboratory or in a large area outside the facilities.

People suffering from knee osteoarthritis may present different values at the time of being studied, since this is because the disease in each person is at a different stage, which was diagnosed by a health professional as mild for the older adult P3, severe for the older adult P2 and moderate for the older adult P1, obtaining error values ranging from 6.36E–10º to 1.18E–05º and correlation coefficients ranging from –0.27 to 0.11, in comparison with data performed by Calderón and Ulloa (2016).

The values obtained in the evaluation determine that older adults comprise a similar pattern which can be distinctive for knee osteoarthritis disease, whereby the angular displacement of the right quadriceps has a maximum angle of 20º and a minimum angle of –103.30º. The angular displacement of the left quadriceps has a maximum angle of 13º and a minimum angle of –130.6º. In pelvic obliquity, there is a maximum angle of 59.6º and a minimum angle of –177.9º. In pelvic rotation, there is a maximum angle of 34.24º and a minimum angle of –67.37º. In the angular displacement of the right tibial, there is a maximum angle of 31.85º and a minimum angle of –176.3º. The angular displacement of the left tibial has a maximum angle of 22.05º and a minimum angle of –179.6º. The angular displacement of the right knee has a maximum angle of 206.3º and a minimum angle of –41.41º. The angular displacement of the left knee has a maximum angle of 155.8° and a minimum angle of –55.23°. The angular displacement of the right ankle has a maximum angle of 27.39º and a minimum angle of –69.59º. The angular displacement of the left ankle has a maximum angle of 25.58º and a minimum angle of –64º.

The gait pattern, in addition to being affected by knee osteoarthritis, can be altered by causes such as overweight, size, footwear, hormonal pathologies and fractures, and trauma, taking as a reference the older adult P2 who in addition to having severe knee osteoarthritis suffers from hormonal pathologies such as hyperthyroidism involving overweight, resulting in a determination coefficient of 0.49 % in pelvic obliquity, 0.84 % in knee flexion and extension for the older adult P1 who has a history of fractures and trauma, overweight having a value of 0.31 % in flexion and extension of the left anterior tibialis anterior.

The comparison made with the Calderón and Ulloa (2016) database does not have the data for the determination of characteristic curves about the left and right foot, for which reason it is not possible to determine the values for the left and right foot.

References

Aranda Valera, I. C., Mata Perdigón, F.J., Martínez Sánchez, I., González Navas, C., Collantes Estévez, E., & Garrido Castro, J. L. (2018). Utilización de sensores inerciales para la evaluación de la movilidad espinal en pacientes con espondiloartritis axial. *Rehabilitación*, *52*(2), 100-106.

Armas, Y. M., Cabrera, V. H., & López, A. (2023). Evaluation of Biomechanical Conditions in Infants from 20 to 48 Months of Age in Gait. In *Intelligent Technologies: Design and Applications for Society, Proceedings of CITIS 2022*, LNNS 607 (pp. 3-12). https://n9.cl/zqb9i0/

Calderón, M., & Ulloa, R. (2016). Cambios asociados al envejecimiento normal en los parámetros angulares de la marcha a una velocidad controlada. *Revista Médica Chile, 144*(1).

Carmenate Milián, L., Moncada Chévez, F. A., & Borjas Leiva, E. W. (2014). *Manual de medidas antropométricas,* 1.ª ed. SALTRA.

Cleland, B. T., Arshad, H., & Madhavan, S. (2019). Concurrent validity of the GAITRite electronic walkway and the 10–m walk test for measurement of walking speed after stroke. *Gait and Posture, 68*, 458-460.

Costa, O., Aubin, A., Oliviera, C., Paz, J., & Luján, C. (2015). Métodos de evaluación de la composición corporal: una revisión actualizada de descripción, aplicación, ventajas y desventajas. *Archivos de Medicina del Deporte, 32*(6), 387-394.

Di, G. T. (2020, 7 marzo). *Plexofisioterapia*, www.plexofisioterapia.es. Accedido el 18 de diciembre de 2023.

Garza-Ulloa, J. (2018). Diseño de experimentos, adquisición de datos y procesamiento de señales. *Researchgate, 1*(4), 179-237.

Góngora García, L., Rosales García, C., González Fuentes, I., & Pujals Victoria, N. (2003). *Articulación de la rodilla y su mecánica articular*. Medisan.

INEC. (2010, 12 septiembre). *Proyección por provincias, sexo y áreas 2012-2020.* https://n9.cl/i1x8/

Jouybari, A., Amiri, H., Ardalan, A., & Zahraee, N. (2019). Comparación de métodos para la determinación de la actitud de una boya ligera mediante datos brutos de IMU. *SAO*, *135*, 348-354.

Martínez, S., Vergara, L., Ramírez, B., & Olmoz, L. (2018). Aplicación de sensores inerciales para análisis de marcha humana. *Revista de Ingeniería Tecnológica*, pp. 23-31.

Moreta, G., Ortega, D., & Cabrera, V. H. (2023). Evaluation of Biomechanical Conditions in Infants from 20 to 48 Months of Age in Gait. *In Intelligent Technologies: Design and Applications for Society, Proceedings of CITIS 2022,* LNNS 607 (pp. 13-23). https://doi.org/10.1007/978-3-031-24327-1_2

Nikaido Y, Urakami H, Akisue T, Okada Y, Katsuta N, Kawami Y, Ikeji T, Kuroda K, Hinoshita T, Ohno H, Kajimoto Y, Saura R. (2019). Associations among falls, gait variability, and balance function in idiopathic normal pressure hydrocephalus. *Clinical Neurology and Neurosurgery, 183.* https://n9.cl/gvj2y/

Panebianco, G. P., Bisi, M. C., Stagni, R., & Fantozzi, S. (2020). Timing estimation for gait in water from inertial sensor measurements: Analysis of the performance of 17 algorithms. *Computer Methods and Programs in Biomedicine, 197.*

Renata, D. S., Fabrice, D. C., Pierre, S., Arnaud, C., Jonathan, C., Sylvie, G., & Jean, C. (2012). Computerized video analysis of social interactions in mice. *Pulmed.gob,* pp. 410-7.

Straw, A., Branson, K., Neumann, T., & Dickinson, M. (2010, 14 july). *Multi-camera real-time three-dimensional tracking of multiple flying animals*. The Royal Society.